ISSN 1070-3632, Russian Journal of General Chemistry, 2013, Vol. 83, No. 11, pp. 2182–2194. © Pleiades Publishing, Ltd., 2013.
Original Russian Text © O.D. Volpian, A.I. Kuzmichev, 2012, published in Rossiiskii Khimicheskii Zhurnal, 2012, Vol. 56, Nos. 1–2, pp. 58–69.

Nanogradient Optical Coatings

O. D. Volpian[a,b] and A. I. Kuzmichev[c]

[a] *Stelmakh Polyus Research Institute State Unitary Enterprise, ul. Vvedenskogo 3, Moscow, 117342 Russia*
e-mail: o.d.volpian@mail.ru

[b] *Scientific-Manufacturing Enterprise "Fotron-Auto Ltd.", Novodanilovskaya Naberezhnaya 8, Moscow, 117105 Russia*

[c] *Kiev Polytechnic Institute National Technical University of Ukraine, Prospect Peremogy 37, Kiev, 03056 Ukraine*
e-mail: A.Kuzmichev@edd.ntu-kpi.kiev.ua

Received June 1, 2012

Abstract—Basic optical coatings with refractive-index gradient along the light propagation direction, structures of gradient coatings, and technology of their manufacturing are considered. Issues relating to longitudinal-nanogradient coatings are discussed.

DOI: 10.1134/S1070363213110388

INTRODUCTION

Optical coatings are an important element of optical and optoelectronic devices. They are applied for matching optical media and controlling light radiation by varying its propagation direction, spectrum, amplitude, phase, or polarization.

Optical coatings consist of one or a great number (up to 200!) of layers with different refractive indices; in the latter case, we deal with a system of layers, in which the refractive index changes stepwise in going from one layer to another. Such systems of layers with alternating low n_l and high n_h refractive indices are used, for example, as interference filters, mirrors, or antireflection coatings. Having appropriataly chosen of materials and thicknesses of individual layers, one can obtain optical systems with excellent characteristics but only in narrow ranges of light wavelengths and incidence angles. Therewith, the sharp, stepwise change of refractive index negatively affects both mechanical and thermal stability and laser damage resistance.

Optical coatings always show certain nonuniformity in the distribution of refractive index due to some specific features of the material, imperfect fabrication technology, or other reasons. Such coatings are called inhomogeneous coatings. Coatings with predesigned smooth inhomogeneity, so-called gradient coatings, have refractive indices which continuously change either with radius [$n(r)$] or with thickness [$n(z)$], but, generally, in all coordinates. Coatings with the $n(r)$ function create a lens effect. They are applied in laser resonators, gradient-index optical devices (GRIN optics), and waveguides [1]. Coatings with the refractive index changing with thickness [$n(z)$ function] along the light propagation direction are called longitudinal-gradient coatings [2]. Figure 1 shows the light pathways in a uniform one-layer coating and in a longitudinal-gradient coating. The refractive index n of the upper layer of the gradient coating is equal to that of the upper medium, whereas the n of the lower layer is equal to that of the support.

Coatings with a longitudinal gradient profile have been known since XIX century. Rayleigh showed in his study on light propagation in the atmosphere that layers with a gradient change of n exhibit antireflection properties in a broad light band. Similar layers were also observed by Fraunhofer. Therefore, even though uniform coatings are most commonly used in optics, and much effort is taken to improve their uniformity,

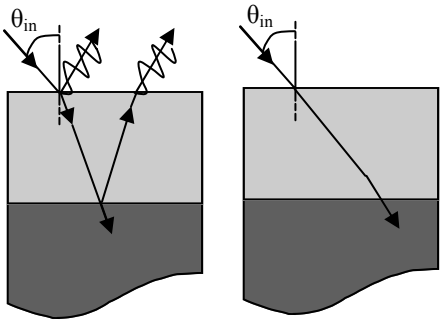

Fig. 1. Path of the beam incident at an angle θ_{in} on (left) uniform and (right) gradient optical coatings.

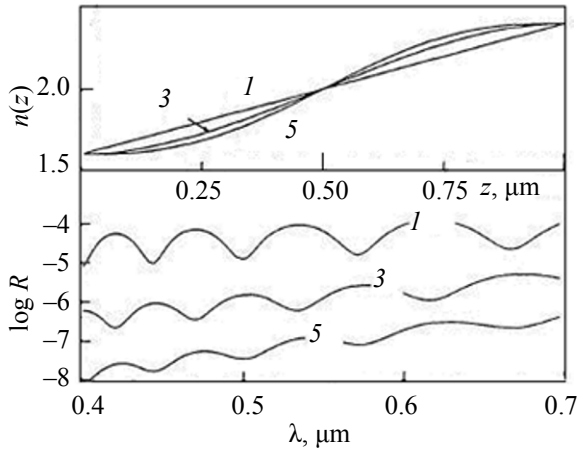

Fig. 2. Refractive-index profiles $n(z)$ in a 1-μm gradient film between two media with $n = 1.6$ and $n = 2.4$ and their corresponding reflection spectra. The reflectivity R without the optical coating is 4×10^{-4}. The figures in the curves relate to the degree of the approximating polynomial. Adapted from [8].

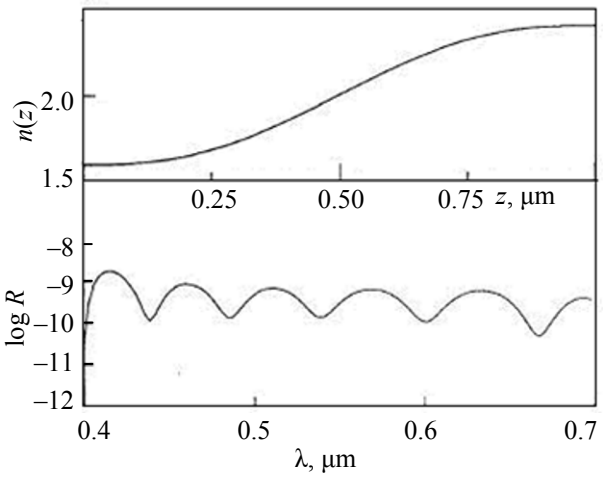

Fig. 3. Result of the optimization of the quintic $n(z)$ profile in Fig. 2 after 30 iterations. Adapted from [8].

gradient coatings still attract interest owing to their potentially higher characteristics. However, the application of gradient coatings is limited by the complexity of technology and high cost of their fabrication. Nevertheless, these problems are being solved to success. In particular, successful fabrication of mechanical, protective, and thermal barrier gradient coatings has been reported [3–7].

In the present work we discuss advances in the fabrication technologies of optical coatings with a longitudinal gradient of refractive index, as well as lines of development of these technologies.

Distribution of Refractive Index in Gradient Optical Coatings

The possible variants of the $n(z)$ distribution in gradient coatings can be divided into monotonically changing n profiles, distributions with an alternating-sign gradient, and hybrid distributions. The choice of one or another $n(z)$ function depends on the destination of the coating, its thickness, and, consequently, possibility of its fabrication. The calculation of gradient coatings with the aim to choose the $n(z)$ function is usually performed by step fitting the gradient $n(z)$ profile: The profile is divided into a great number ($i \geq 60$) of uniform thin layers with the refractive index n_i equal to the average refractive index over the sublayer thickness, and the calculation is continued using procedures for multilayer interference systems.

Let us consider example $n(z)$ distributions.

Monotonic n(z) Distributions

The main purpose of optical coatings with a monotonic $n(z)$ function is to impart antireflection properties to different surfaces. Typical $n(z)$ functions of this group are linear, cubic, and quintic, as well as those fitted by a part of a sine-wave function. The change from a linear to cubic function ensures continuity not only of $n(z)$, but also of the first derivative of n, whereas in the case of a quintic function, the second derivative of n is also continuous. When $n(z)$ distribution is described by a high-degree polynomial, a lower gradient at coating interfaces, better matching optical media, and, consequently, lower reflection coefficients R can be provided (Fig. 2). In the case of polynomials of degrees higher than 5, the gradient of refractive index in the middle part of the coating increases so strongly that the antireflection effect no longer improves [8]. At the same time, as established by Kim and Lee [9], the reflectivity is best reduced by coatings with the $n(z)$ distribution fitted by a 9th degree polynomial. A prechosen $n(z)$ distribution can be further optimized to improve reflectivity. To this end, the gradient layer of the optical coating is divided into a great number of uniform thin layers with the n_i changing stepwise from layer to layer so that the $n(z)$ approximation is continuous. Fifteen sublayers at $\lambda/4$ (λ is the incidence light wavelength) would suffice. Further on the n_i for each sublayer are fitted using

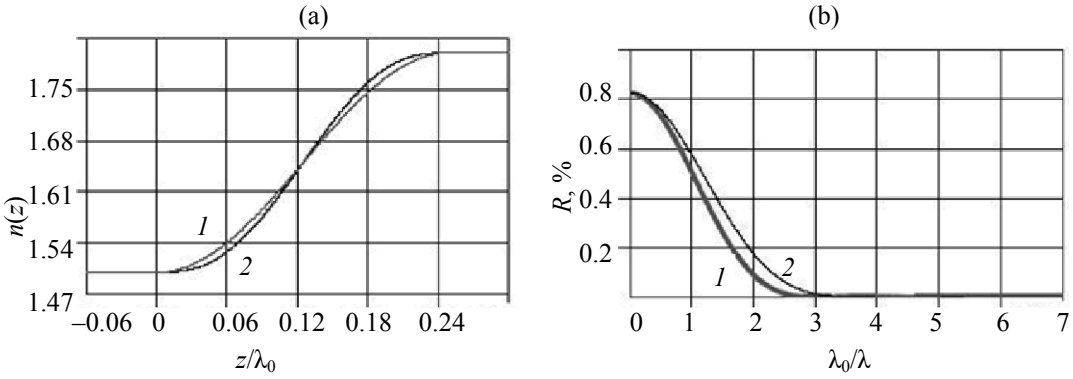

Fig. 4. (a) Gradient $\lambda_0/4$ layer and (b) its reflection spectrum for (*1*) sine-wave and (*2*) quintic $n(z)$ distributions. Adapted from [10].

known procedures for optimization of maultilayer interference systems.

Figure 3 shows the optimization results for 250 sublayers after 30 iterations, beginning with the quintic distribution presented in Fig. 2. As seen, an essential reflectivity reduction over the entire visible range takes place already at minor changes in the initial $n(z)$ distribution and the coating thickness of 1 μm. In [9], evidence was obtained showing that the optimization of $n(z)$ with a combination of an algebraic and a sine-wave functions allows the visible-light reflectivity to be reduced to 10^{-12} even if the coating thickness is 0.7 μm.

Let us now dwell on the theoretical prerequisites of the effect of antireflective band broadening in going to a gradient $n(z)$ distribution in the case of a highly refractive substrate. Consider an equivalent as a multilayer system. A $\lambda_0/4$ coating with its corresponding n gives an excellent result for one wavelength λ_0. As further layers are added to this system, the anti-reflective band broadens, and the refraction coefficient R in the band decreases. In a limit, we will have an infinite number of layers with an infinitely small difference in n_i for neighboring layers. However, if, on adding layers, we do not change the total optical thickness of the multilayer system, the thickness of individual layers will tend to zero, and the system in whole will in practice represent a monolayer with the same optical thickness but with its refractive index n changing continuously from the substrate to the top layer.

Let a multilayer system contains m layers with the total optical thickness $T = m\lambda_0/4$. Then we have m spectral points with zero reflection in the range from λ_1 to λ_2:

$$\lambda_1 = [(m+1)/m]\times\lambda_0/2 = 2[(m+1)/m^2]\times T,$$
$$\lambda_2 = (m+1)\times\lambda_0/2 = 2[(m+1)/m]\times T$$

At the wavelengths $\geq \lambda_2$, no antireflection effect can be attained [10]. If m is increased to infinity but T is left the same, we obtain a single gradient layer with $\lambda_1 \to 0$ and $\lambda_2 \to T$. All waves with the length λ will not be reflected in this range. Thus, a nonuniform layer with monotonically changing refractive index will serve as an excellent antireflective coating for wavelengths shorter than the double optical thickness. At high wavelengths, reflection appears, while at $\lambda > 4T$ the coating becomes quite inefficient.

With antireflective gradient coatings, the problem of their matching the refractive index of the coating to that of air arises. This problem is associated with the lack of natural materials with $n = 1$, for fabrication of the top layer of the coating, which is contacting with air. This problem is solved by using porous inorganic and polymeric materials.

Alternating-Sign Gradient n(z) Distributions

The coatings with such $n(z)$ distributions serve as narrow-band reflection (block, reject) filters or, as they also called, notch filters. The $n(z)$ distribution in such filters has a sine-wave pattern, and, therefore, in English-language literature they are referred to as *rugate* filters.

Notch filters are usually fabricated from $\lambda_0/4$ systems with uniform layers, but such systems reflect at many other wavelengths than λ_0: $\lambda_0/3$, $\lambda_0/5$, $\lambda_0/7$, etc. This problem can be solved by implementing the $\lambda_0/4$ layer as a gradient layer as shown in Fig. 4a. Actually, the spectrum in Fig. 4b shows no reflections apart from the reflection at the principal wavelength.

Increased number of $\lambda_0/4$ layers in a notch filter does not decrease the number of reflection bands but

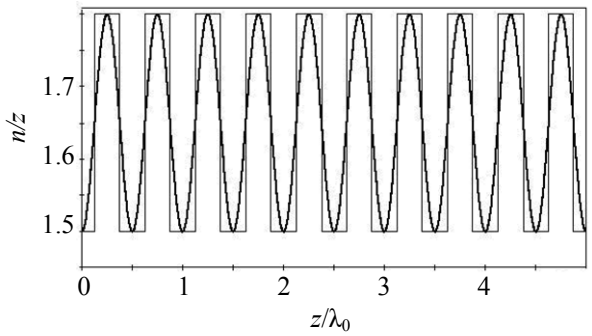

Fig. 5. Replacement of the step rectangular refractive-index profile of a rugate notch filter by a gradient (sine-wave) profile.

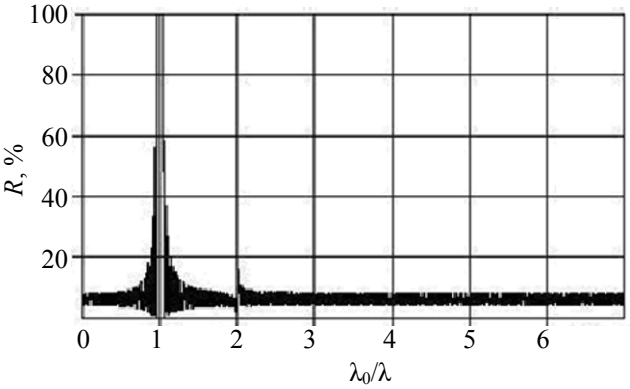

Fig. 6. Reflection spectrum of the rugate notch filter with the structure shown in Fig. 5. Adapted from [10].

only makes them narrower. Therefore, to suppress higher order bands, each $\lambda_0/4$ layer in the filter should be made gradient, both at the n ascend and descend fronts, i.e. the step rectangular profile should be replaced by a sine-wave one (Fig. 5). Figure 6 demonstrates the result of such a replacement: The spectrum of a rugate filter has only one, strong and narrow band. Some noise at the band feet is explained by a limited number of layers in the coating. Clarification of the reflection spectrum from sideband lobes and noise can be attained by apodization (modification, modulation) of the shape of the envelope function of the rugate filter as shown in Fig. 7 (bottom drawings).

The technology of fabrication of alternating-sign gradient rugate filters should be much more complicated compared with that for single-layer gradient antireflection coatings. A reasonable approach to this problem is likely to involve an approximation as a sequence of uniform layers with a step gradient of refractive index. By analogy with the dc-to-ac sine-wave power conversion in pulse techniques, approaches based on amplitude–pulse, width–pulse, and phase (frequency)–pulse modulation are used; the same approaches can also be realized in the technology of gradient coatings.

According to the first approach, a continuous $n(z)$ profile should be replaced by a sequence of ascending and descending steps. Each step will represent a uniform sublayer with the refractive index n_i equal to the half-sum of the refractive indices at its edges in the continuous $n(z)$ profile. The thickness of individual layers should be much smaller than $\lambda_0/4$. If sublayers will be thick (i.e. they will be less in number), higher order bands will appear in the reflection spectrum, and the main refection band will get broader.

According to the second approach, the heights of n_i steps are fixed, but the width of sublayers will be varied so that the mean $\langle n_i \rangle$ value in the ranges "step with a high n_h – valley with a low n_l" changes like $n(z)$ in a gradient coating. The third approach involves variation of the widths of sublayers (valleys) with low n_l values at fixed step heights and widths of sublayers with high n_i values. The latter two approaches are easier to realize, but the corresponding reflection spectra show broad higher order bands. For their suppression the number of sublayers per $\lambda_0/4$ should be much increased.

The above-considered approximations are useful not only for designing fabrication technologies for rugate filters but also for calculations by the procedures for multilayer interference coatings.

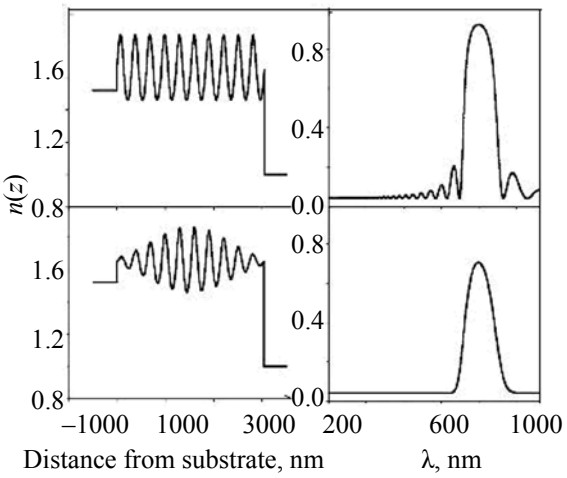

Fig. 7. (Bottom drawings) Apodization of the envelope function of a rugate notch filter for improving its reflection spectrum.

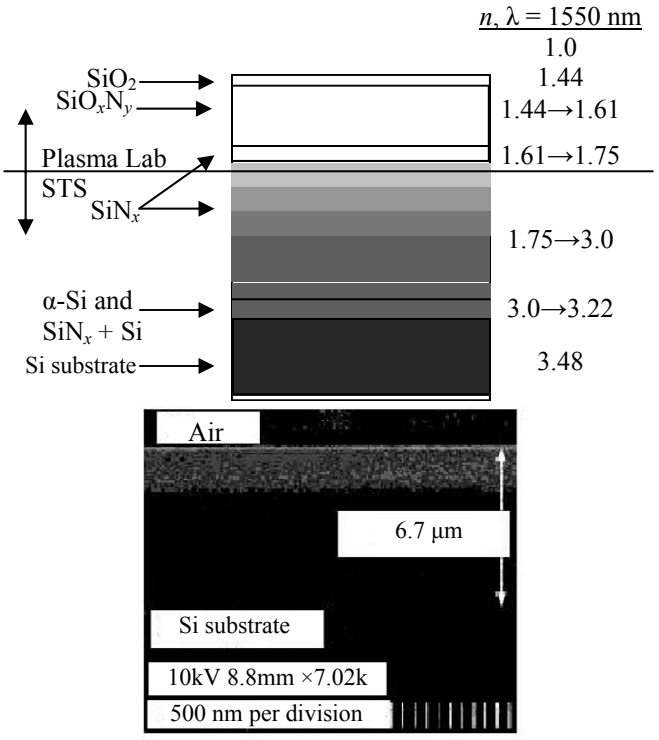

Fig. 8. Multilayer gradient antireflective coating with a dense microstructure, fabricated by plasma vapor deposition. (Bottom) Electron microscope image of the vertical section of the coating. Adapted from [15].

Hybrid n(z) Distributions

Along with coatings with monotonic and alternating-sign $n(z)$ gradients, coatings (for example, antireflective) combining uniform and nonuniform layers can be created [11, 12]. Design of their fabrication technologies, as well as their modeling are performed by step approximation of $n(z)$ with division of gradient parts of the coating into thin uniform sublayers. The results of such approaches to the fabrication (electron-beam vapor deposition and magnetron and ion-beam sputter deposition) and modeling of coatings fairly agree with each other [11, 12].

Features of the Nanostructure of Gradient Coatings

A longitudinal gradient of refractive index is created by continuously varying the chemical composition of the coating substance. Such variation can be performed in different ways to form gradient coatings with different nanostructures. The refractive index of such coatings is controlled on the basis of the effective medium theory which considers a material of complex composition (composite) as a uniform material with properties which are roughly an average of the properties of its components. Therefore, changing the relative concentrations of components with high n_l and low n_h changes the effective refractive index n. Therewith, the dimensions of the composite components should be much smaller than working wavelengths. This condition is fulfilled when the components mix at the same molecular level, for example, to form a solid solution, or when the components are used as nanoblocks, for example, as loosely packed nanorods.

Most commonly, Si oxide→oxynitride→nitride and Si oxide–metal oxide systems are used. Other compositions are also possible (for example, Zr oxide–Mg fluoride system [13]), as well as binary compounds of a metastable nonstoichiometric composition, having different refractive indices (for example, Mo oxides [14]). Such compositions, when deposited by a corresponding technology involving mixing at the molecular level, form gradient coatings with a dense low-pore microstructure. Figure 8 shows an example of a broad-band gradient dense dielectric antireflective coating containing layers of amorphous α-Si and Si nitrides, oxynitrides, and oxides.

Coatings with a dense nonporous microstructure are resistant to environmental factors, first of all humidity, chemical, mechanical, and thermal effects, contamination, as well as laser-induced damage. Therefore, such coatings are of particular interest for fabrication of fail-safe optical and laser devices.

In view of the fact that there are almost no substances in the nature dense enough for their refractive index to be about 1, i.e. close to the refractive index of air, a problem arises to obtain a coating whose $n(z)$ function changes continuously from 1 to a value equal to the refractive index of the substrate.

This problem can be approached analogously to the above-described case, namely, the coating is fabricated from a solid refractive substance with pores filled with air: Porosity is a maximum at the coating–air interface (up to 85–95 %) and a minimum near the substrate, and, therefore, the coating and substrate materials will have close or even coincident n values. Such coatings are most frequently fabricated from silicon and silicon oxide, as well as from indium–tin oxides (ITO), GaP, etc.

Figures 9 and 10 provide examples of porous structures consisting of inclined nanorods. These

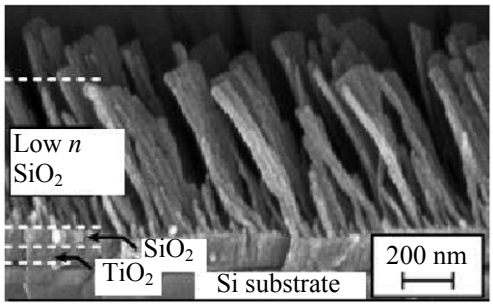

Fig. 9. Gradient coating with a porous rod-shaped structure of upper layers. Adapted from [17].

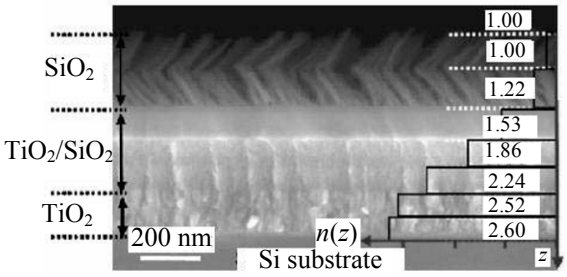

Fig. 10. Gradient coating with a rod-shaped structure of upper layers [18]. The zig-zag was obtained by varying the vapor incidence angle on the substrate. Adapted from [18].

structures were formed by oblique-angle vapor deposition onto fixed substrates [Glancing Angle Deposition (GLAD) technology]. In the case of SiO_2 nanorods, the coatings deposited by the GLAD technology had a very low refractive index (n = 1.08) [16].

The gradient refractive index in such structures is obtained by varying the incidence angle of condensing particles on the substrate. Due to the self-shielding effect which occurs when particles are deposited at a low substrate temperature (i.e. in the absence of surface diffusion of deposited particles), increasing the particle incidence angle enhances shielding of the substrate surface and porosity of the coating. The lowest porosity and the highest refractive index form in that part of the coating, where particles are deposited at a normal incidence angle.

With a spinning substrate, vertically oriented nanorods can be obtained (Fig. 11a), since spinning allows axially symmetric condensation. The resulting axially symmetric structures lack birefringence typical of systems with inclined nanorods. Figure 11b shows a scheme of controlling the thickness and, consequently, refractive index of the nanorod layer. Such a gradient antireflective SiO_2 nanorod coating shows a more than 99 % transmittance in the visible and near-UV spectral ranges.

The structure of gradient coatings consisting of discrete nanoblocks or nanoelements can be formed not only of nanorods, but also of elements of any other shape, including cones, pyramids, or nanospheres (for example, of SiO_2). Discrete nanoelements can be implemented as holes in a substrate; one can, say, impart the holes a cone shape to reduce the refractive index near the surface contacting with air. Gradient optical structures can be fabricated not only of commonly used inorganic materials, but also of polymers [20].

For gradient coatings with a discrete/porous structure to function with a minimum light scattering over a wide wavelength range, the following condition should be fulfilled: Inhomogeneities in the coating (nanoprotrusions and crevices between them, or nanopores) should be much smaller in size than the

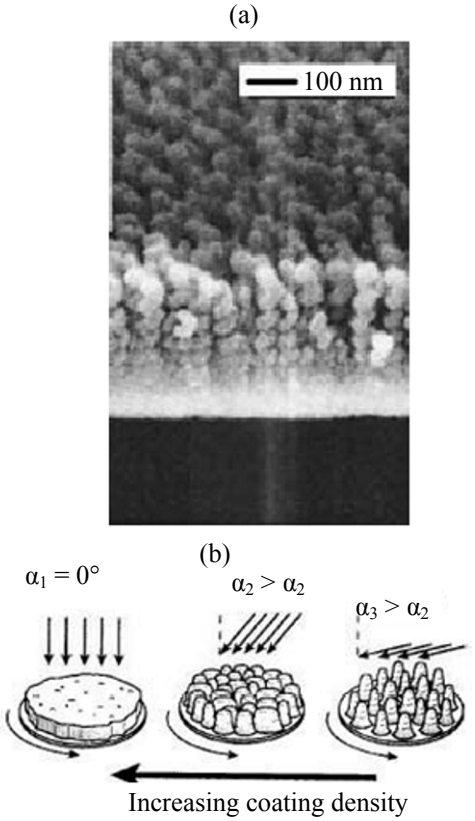

Fig. 11. (a) Gradient coating with a porous axially symmetric nanorod structure and (b) scheme of refractive-index control. (α) Incidence angle of coating particles on the support. Adapted from [19].

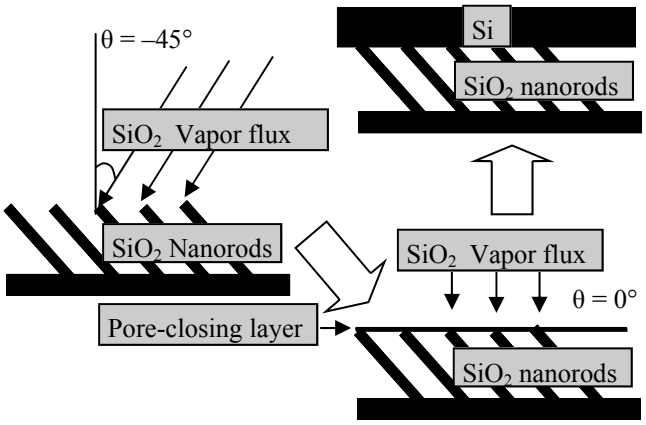

Fig. 12. Schematics of the process of pore closure in a coating. Adapted from [16].

working wavelengths, i.e. they should be of a nanoscale size.

To extend the range of variation of refractive indices in gradient coatings, layers having different microstructures are combined, as, for example, in an almost ideal antireflective coating for silicon solar cells (Fig. 10). Here the top two layers which are contacting with air consist of randomly distributed nanorods deposited by the GLAD technology with electron-beam evaporation of SiO_2 granules to obtain $n \approx 1$. The following three layers obtained by co-sputtering of Ti and Si oxide combinations have a relatively low-pore structure. Finally, the two dense layers next to the substrate are made of Ti oxide. This coating reduces reflection of the visible and near-IR range by 42.7 % compared with a noncoated surface [18].

There is an obvious essential drawback of porous optical coatings: They are sensitive to environmental factors; specifically, moisture and other substances, including dirt, can penetrate into pores; mechanical exposures can damage nanorods on the surface, or porous structure can be destroyed by high temperatures. All this leads to uncontrolled changes in the refractive index of the coating material. Porous structures can have decreased laser- or plasma-induced damage thresholds. Various approaches were proposed to minimize these drawbacks. The main technique involves closing pores on the outer coating surface. The scheme of this process is shown in Fig. 12.

The GLAD technology with electron-beam evaporation is used to deposit a layer of inclined SiO_2 nanorods, after which the substrate is turned, and a thin layer (20 nm) of SiO_2 nanorods is deposited at a negative θ angle to close pores in the lower layer (a zig-zag structure is formed). Then a 41-nm-thick Si layer is deposited at a normal incidence angle. The latter layer finally closes pores and forms the top, functional layer of the coating.

To conclude our consideration of nanoporous coatings, we would like to note that the first gradient coatings were implemented just as nanoporous structures: It was way back when Fraunhofer obtained such coatings by etching glass plates in acids. Note also that optical systems like gradient coatings, formed by protrusions, exist on the eye surface of some insects, for example, moth, i.e. these coatings are biomimetic. Microprotrusions, or, more likely, nanoprotrusions, form a heterogeneous density-gradient medium on moth eye; this much reduces reflection in wide ranges of wavelengths and incidence angles, and, therefore, insects can see even in the dark. Moreover, gradient structures are sometimes fabricated using replicas (masks) obtained from eyes of insects, for example, flies.

Fabrication of Gradient Optical Coatings

The choice of technology for fabrication of a gradient coating depends on its expected microstructure and characteristics.

Fabrication of Coatings of Discrete Nanoelements

Below we consider the technologies for fabrication of gradient coatings consisting of 3D discrete nanoelements whose configurations are described in the previous section.

Nanoelements in the form of pores in the substrate are fabricated by chemical, electrochemical, and reactive ion etching (such technologies are well developed for leaching glass and obtaining nanoporous Si; thus a porous silicon coating as little as 100 nm thick, which reflected less than 5 % in the wavelength range of 0.4–1 μm, was created [15]).

Gradient coatings with bulky nanoelements on the outer substrate surface (like those shown in Figs. 9–12) are fabricated by the GLAD technology with high-vacuum electron-beam evaporation for a maximum self-shielding of condensing particles [19], as well as by chemical technologies of deposition and treatment of gradient-porous polymer films [20]. Note that the sol–gel technology which is frequently mentioned in terms of the fabrication of nanoporous materials is hardly suitable for gradient optical coatings because it

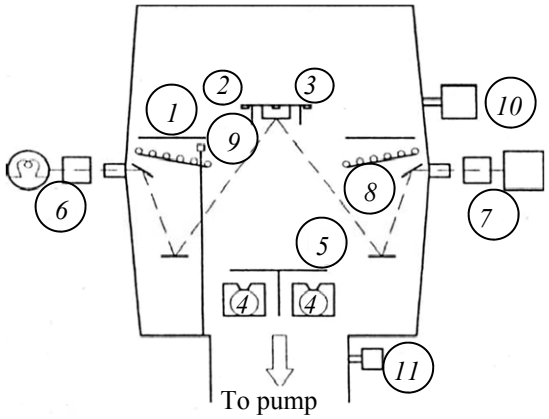

Fig. 13. Schematic of an electron-beam evaporation setup [13]: (*1*) six substrate holders; (*2, 3*) quartz microbalances; (*4*) electron-beam evaporators; (*5*) shutter valve; (*6–7*) optical monitor comprising (*6*) light source with shutter and (*7*) monochromator with detector; (*8*) substrate heaters; (*9*) temperature sensor; (*10*) residual gas analyzer; and (*11*) gauge.

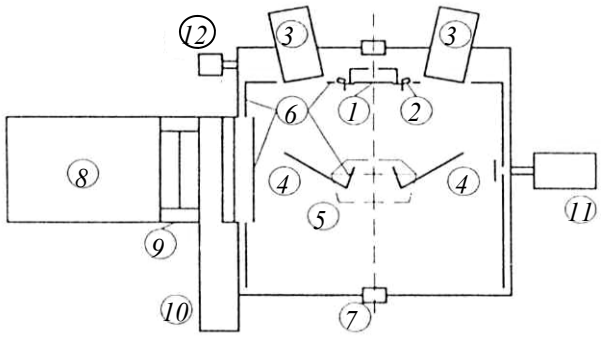

Fig. 14. Schematic of an ion-beam sputtering setup [13]: (*1*) substrate; (*2*) quartz microbalances; (*3*) Kaufman ion sources; (*4*) targets; (*5*) ion source directed to the substrate; (*6*) screens around the chamber and between targets; (*7*) optical monitor; (*8*) cryogenic pump; (*9*) throttle valve; (*10*) shutter; (*11*) residual gas analyzer; and (*12*) gauge.

is hardly able to ensure a reproductible thickness and transverse uniformity of deposited films.

Fabrication of Dense Nanostructured Coatings

Dense nanostructured coatings are fabricated by technologies well-proven in microelectronics and in the fabrication of traditional optical coatings, namely, chemical vapor deposition (CVD) and physical vapor deposition (PVD) in those versions which allow one to obtain coatings with a chemically variable composition at comparatively low substrate temperatures. To this end, the usual high-temperature CVD is replaced by low-temperature plasma-enhanced deposition (PE CVD).

PE CVD technologies. Plasma is generated by means of RF discharge in a two-electrode (condensator) system at a frequency of 13.56 MHz or in the dual-frequency mode [21–23] or microwave discharge in the electron-cyclotron resonance mode in an electrodeless system at a frequency of 2.45 GHz [24].

Gradient coatings of amorphous silicon oxynitride SiO_xN_y and a SiO_2/TiO_2 mixture were fabricated in a RF system [21–23]. The starting materials in the first case were gaseous SiH_4, N_2O, and NH_3 (total pressure 10.6 Pa, constant SiH_4 flow rate, computer-controlled N_2O and NH_3 flow rates). The SiO_2/TiO_2 mixture was prepared using O_2 (constant flow rate) and $TiCl_4$ and $SiCl_4$ vapors with controlled flow rates; total pressure 3.6–6.6 Pa; discharge power 100 W; negative auto-offset voltage at the substrate ca. 400 V. The ranges of variation of the refractive index of the coating were 1.46–1.86 for SiO_xN_y and 1.46–2.35 for SiO_2/TiO_2. The deposition rate depended on the composition of the gas mixture and comprised ~ 0.7 nm s^{-1} for SiO_xN_y and ~1.3 nm s^{-1} for the oxide mixture. The RF system [21–23] was tested in the fabrication of single- and multiband rugate filters. The deposition time of the filters at their total thickness of a few micrometers is about several hours.

Figure 8 shows the structure of the gradient coating fabricated by the PE CVD technology using two plasma systems: STS ($SiH_4 \rightarrow$ α-Si, $SiH_4+NH_3 \rightarrow SiN_x$) and Plasma Lab ($SiH_4+N_2O+NH_3 \rightarrow SiO_xN_y$) [15].

Callard et al. [24] used the microwave technology for fabricating gradient silicon oxynitride coatings from SiH_4, O_2, and N_2. The SiH_4 and N_2 flow rates were maintained constant (4 and 20 sccm, respectively), while the flow rate of O_2 (as the most active gas) was varied in the range 0.5–8 sccm; total pressure 0.2 Pa; discharge power 220 W; substrate temperature 200°C. Under these conditions, gradient coatings with a linear and a parabolic variation of refractive indices were fabricated (film thickness 300 nm, SiO_2 volume fraction 46–96%, deposition time ~ 1.5 h).

PVD technologies. Gradient coatings are fabricated using physical deposition technologies. However, since a reactive gas (O_2 and/or N_2) is always fed to the reaction chamber, these technologies always involve chemical processes.

(1) Co-evaporation of two materials, one with low n_l and the other with a high n_h, by electron beams [electron-beam evaporation (EBE)] [25]. This technology was used to fabricate double-band rugate notch (reflective) filters (composition SiO_2/TiO_2; varied rate of TiO_2 evaporation) [26], as well as an antireflective coating (composition ZrO_2/MgF_2; varied rates of evaporation of both materials; deposition rate ca. 1 nm s^{-1}; substrate temperature 80°C; the scheme of the setup is shown in Fig. 13).

(2) Co-sputtering of two materials, one with low n_l and the other with a high n_h, by ion beams [ion-beam sputtering (IBS)]; one beam can be used to sputter both materials. Ouellette et al. [13] used this technology to fabricate rugate notch filters (composition SiO_2/TiO_2; varied TiO_2 sputtering rate; film thickness 30 μm, deposition time 104 h; the scheme of the setup is shown in Fig. 14).

(3) Co-sputtering of two materials, one with low n_l and the other with high n_h, by means of two magnetron sputtering systems.

(4) Magnetron sputtering of silicon at a varied composition of the gaseous reaction mixture (O_2+N_2). This technology was used to fabricate a SiO_xN_y film.

(5) Magnetron sputtering of molybdenum in an oxygen medium was used to fabricate metastable MoO_x gradient films under the conditions of varied magnetron discharge power [14].

Target values of refractive indices in the co-evaporation and co-sputtering technologies are attained by selecting the deposition rate ratio of coating components. The required deposition rate ratio of the low-n_l (D_l) and high-n_h (D_h) components can estimated by the following formula [26]:

$$D_l/D_h = (n_h^2–n^2)/(n^2–n_l^2).$$

In connection with technologies 1 and 2, we can also mention ion assisted deposition (IAD) and ion beam–assisted deposition (IBAD), which include electron-beam evaporation or ion-beam sputtering with ion bombardment of the surface of the layer being deposited. The source of ions in IAD is plasma generated in the vicinity of the substrate and in IBAD, a special ion source (ion gun). Ion assistance not only serves for ionic cleaning of the condensation surface before deposition of a coating substance, but also for treatment of the condensate itself with the aim to enhance adhesion, thicken the nanostructure, and stimulate the chemical synthesis of the coating material.

The scheme in Fig. 14 exemplifies the process of ion assistance in the IBAD IBS technology. The setup is complemented by an ion source directed to the substrate. A mixture of Ar and O_2 is fed to the source. Due to ion bombardment and the gradient profile of refractive index of the fabricated notch filter (SiO_2/TiO_2 coating), the optical and mechanical properties of the latter and its resistance to the environment are higher of or at least compare with those of usual multilayer coatings [13].

Lambrinos et al. [27] realized the IBAD IBS process to fabricate an amorphous silicon oxynitride film. The Si_3N_4 target is sputtered by means of N_2^+ ions in an O_2+N_2 mixture at room temperature. The Si_3N_4 : SiO_2 ratio (SiO_2 is formed by Si oxidation after Si_3N_4 dissociation) is controlled by varying the O_2 fraction in the medium and the intensity of substrate bombardment with N_2^+ ions with the energy of 200 eV (the SiO_2 fraction increases with increasing N^+/Si arrival ratio).

Snyder et al. [28] explored the process of fabrication of a gradient Si oxynitride coating on a silicon substrate by the IBAD EBE technology in a Balzers-760 setup. Silicon is evaporated under electron beam in an oxygen atmosphere, and nitrogen ions generated in a Kaufman source (current 100 mA, energy 500 eV) are directed to the substrate, the N^+/Si ratio is 1 : 1. The chemical composition of the condensate is controlled by varying the N_2 and O fluxes fed to the chamber.

The IAD EBE process was realized on a Leybold Syrus-Pro deposition system to fabricate gradient coatings (rugate notch filters). Two electron guns were used to evaporate Nb_2O_5 and SiO_2 with assistance of ions from plasma generated with an advanced plasma source (APS) [29]. This technology for fabrication of gradient coatings (controlling the composition of the coating by varying the evaporation rates of the components; deposition rate ≈ 1.4 nm s^{-1}) [11, 12] with the IBS process (Ar^+ ions were sputtered from Si and Ti target in oxygen at a pressure of 0.4 Pa; controlling the composition of the coating by changing the position of the targets with respect to ion beam, deposition rate of a SiO_2+TiO_2 gradient coating 0.02–0.06 nm s^{-1}) and by sputtering ceramic targets (SiO_2 and Ta_2O_5) in a RF magnetron sputtering setup (controlling the composition of the coating by varying

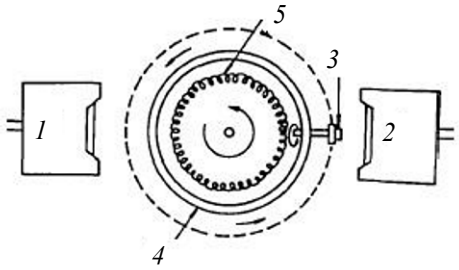

Fig. 15. Schematics of a magnetron sputtering setup [30]: (*1, 2*) magnetrons; (*3*) substrate; (*4*) screen for preventing cross-dusting of targets; and (*5*) heater.

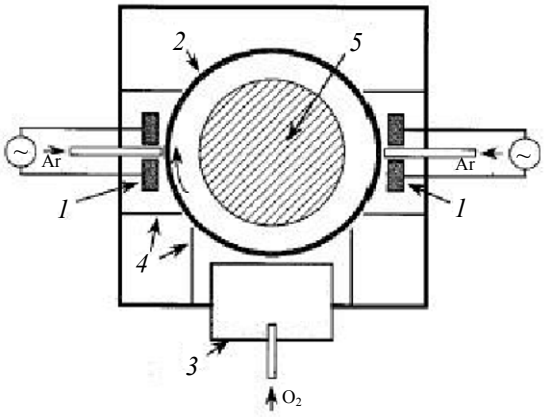

Fig. 16. Schematic of a magnetron sputtering setup with an oxygen activator [32]: (*1*) dual magnetron sputtering systems; (*2*) substrate holder; (*3*) RF oxygen activator; (*4*) screens; and (*5*) pump system.

the power of the setup up to 800 W; Ar volume flow rate 59 sccm, O_2 4 sccm; coating deposition rate ≈ 0.14 nm s^{-1}).

Experimental comparison of the above technologies shows that IBS and magnetron sputtering result in minimum errors: The errors in a preset $n(z)$ distribution are 0.2 and 0.25%, respectively, against 0.6 % for EBE), but the co-evaporation technology provides the highest deposition rate. On this basis we can conclude that the magnetron technology shows the greatest promise, especially if RF sputtering of dielectric targets is replaced by sputtering of conductive targets in the mid-frequency (pulse) mode.

Radio-frequency magnetron sputtering of two targets (Ti and SiO_2) was used to fabricate mixed-composition films [30]. The setup scheme is presented in Fig. 15. The refractive index of the film was controlled by varying the relative power of the magnetron sputters incorporated into a common magnetron sputtering system (maximum power of the magnetrons 400 W). The operating parameters are as follows: deposition rates of pure Ti and Si oxides 12.1×10^{-2} and 18.6×10^{-2} Å min^{-1} W^{-1}, respectively; O_2 fraction in its mixture with Ar 30% at a total pressure of about 4.6 Pa; substrate temperature 85°C. Films with a dense amorphous microstructure and a widely varied composition were obtained.

The films with the refractive index intermediate between those of Ta and Ti oxides were fabricated by *dc* magnetron sputtering of separate Ta and Ti targets in an $Ar+O_2$ mixture [31]. The components of the coating were mixed by alternately turning the substrate to targets; the composition of the coating was controlled by varying the sputtering rates of the targets. Coatings were deposited on the surface of halogen lamp bulbs. The lamps preserved performance at high temperatures.

A more advanced setup with dual magnetron sputtering systems [32] is presented in Fig. 16. Each magnetron sputter comprises two targets (either from Ta or from Si) connected to a low-frequency (pulse) power source. The alternating-sign voltage prevents arc discharges on targets in the reaction gas medium. The substrate holder is spinned at ~100 rpm and moves substrates from one sputter to the other and then to the RF oxygen activator, where previously deposited metal particles are efficiently oxidized to form stoichiometric oxides. A radio-frequency electrodeless plasma discharge with a power of 2 kW is maintained in the activator. Molecular oxygen is excited and ionized here to form reactive oxygen species, and the latter oxidize the metal condensate on substrates. The refractive index of the coating is controlled by varying the supply power of the sputters; maximum sputter powers for the Ta and Si targets are 1.5 and 2.8 kW, respectively. In view of the possibility to smoothly vary the power, a smoothly varied refractive index can be provided (a real gradient coating can thus be obtained).

In this setup, targets are sputtered in the metal mode, which eliminates hysteresis phenomena on the targets, provides a reproducible sputtering rate at a varied sputter power, and a high coating deposition rate (up to 40 nm/min). Gas flow rates: O_2 60 sccm, Ar 300 sccm for Ta, and 200 sccm for Si. Total pressure

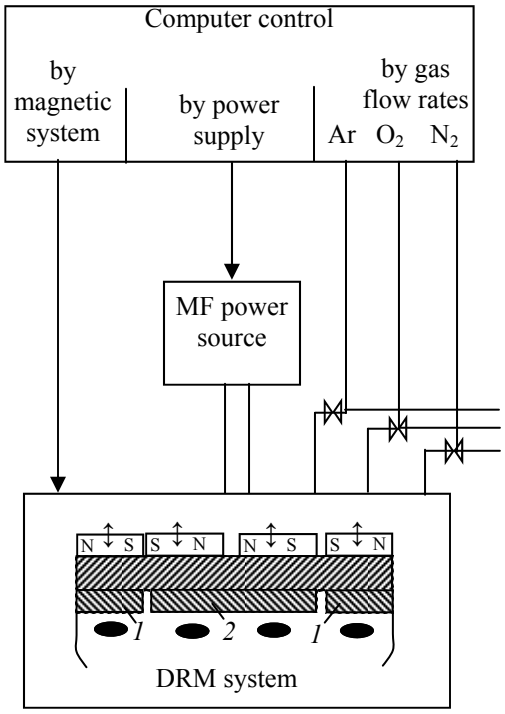

Fig. 17. Schematic of an MF-powered dual magnetron sputtering system for SiO_xN_y deposition: (*1*) outer ring target; (*2*) inner disc target. (Black ellipses) Magnetron discharge plasma. Adapted from [34].

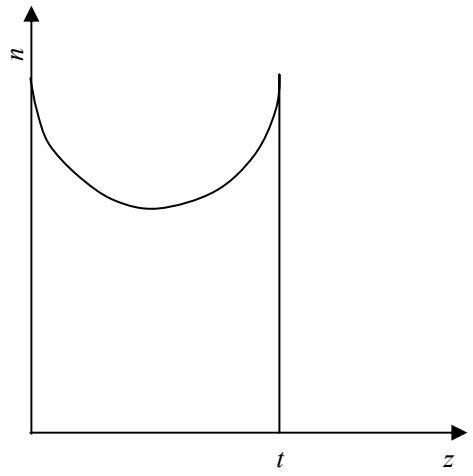

Fig. 18. Nanogradient concave $n(z)$ profile along the light propagation direction ($t \le 100$ nm) for creating a photonic barrier. (t) Barrier coating (layer, film) thickness.

0.5 Pa. Refractive index range 1.463–2.182 at 550 nm. The absorptivity at this wavelength is lower than 5×10^{-4} at $n < 2.0$ and lower than 1×10^{-3} at $n > 2.0$. The technology realized at this setup allows fabrication of coatings with a dense poreless amorphous microstructure.

Song et al. [33] reported the dc magnetron sputter deposition of a mixture of stoichiometric oxides SiO_2+Nb_2O_5 in an analogous setup [33].

Bartzsch and co-workers [34–37] fabricated gradient SiO_xN_y layers by the magnetron sputtering technology: Silicon was sputtered using one dual magnetron system, and the composition and refractive index of the coating were controlled by varying the composition of the reactive gas mixture (O_2+N_2) fed to the system (Fig. 17).

The sputter is a double-ring magnetron (DRM) with an outer ring target (from Si) around a disk target (also from Si). Mid-frequency (MF, tens to hundreds kHz) voltage with alternating polarity is supplied so that the targets work alternately as a cathode and an anode. This prevents arc dischanges on the targets and suppresses the disappearing anode effect (both these effects are associated with the formation of a dielectric oxynitride film on the targets). The pulsed target powering neutralizes the charge on the film and favors its sputtering as the target is working as a cathode. Thus, a dual magnetron system alternately generates a circular discharge above each target.

The MF power supply to the sputter (rate of target sputtering), magnet positions, and gas feed rates are computer-controlled. Argon is used to sputter silicon; oxygen and nitrogen are used to synthesize silicon oxynitride on the substrate surface. The composition of SiO_xN_y is controlled by varying the O_2 and N_2 flow rates. The refractive index of the deposited silicon oxynitride depends on the oxygen fraction in the gas mixture and can be varied from 1.46 to 1.99.

The above-described dual magnetron sputtering system (diameter 400 mm) allows deposition of coatings with a thickness uniformity of ±1% on fixed substrates with diameter of 200 mm. This system was used successfully to deposit layers with a linear or a sine-wave gradient of refractive index for antireflective coatings and rugate notch filters [34–37]. The deposition time of an antireflective coating was ~5 min, and that for a rugate filter with several tens periods is a few hours.

Nanogradient Optical Coatings

Over the past years research's attention has been engaged by coatings whose optical parameters are continuously distributed on the nanometer scale. Such objects can be referred to as nanogradient optical coatings (or even film metamaterials, or metacoatings

[39]). Such materials are considered as candidates for the development of new optical devices, in particular, subwave photonic barriers, filters, polarizers, etc. The theoretical basis of operation of such devices was laid by Shvartsburg and co-workers (see, for example, [38]). In particular, they provided evidence for the existence of nonlocal dispersion in nanogradient structures. Figure 18 shows a variant of the nanostructure of a photonic barrier.

The problem is to develop a technology for fabrication of such coatings, which would be able to ensure a precision growth of a low-defect nanofilm of preset composition. Analysis of different approaches to the fabrication of nanogradient profiles shows that the most suitable technology is the technology of MF (pulsed) magnetron sputtering of several metals (or substoichiometric oxides) in a reactive gas medium of constant composition at a constant sputter power [2]. The latter features of the technology have much in common with those of the above-considered magnetron technologies.

To realize this approach, an automated computer-controlled setup operating in the MF (22 kHz) pulsed sputtering mode [2] has been developed. The setup provides a highly stable and reproducible deposition of mixtures of oxides and fluorides in a reactive gas medium, efficient energetic activation of synthesis of coating material without additional heating of substrate, and high density and minimum roughness of coatings with minimum optical losses. The process is controlled by *in situ* optical monitoring of coating parameters by means of a spec-trovisor (the thickess, refractive index, and current spectral characteristics of the growing film are measured).

This setup was used to fabricate nanogradient optical structures with different refractive-index profiles and modulations. In [2, 39] we presented data on some nanogradient antireflective coatings and meta-coatings which show that the experimental spectra are in a good agreement with calculation. The dispersion dependences of ref-racttive index for a film obtained by Nb and Si sputtering revealed a nonlocal abnormal pattern. Further research into this issue is in progress.

Testing nanogradient coatings for resistance to radiation, climatic factors, and mechanical stresses showed that the coating parameters meet the requirements to elements of optical and laser devices. These properties are largely associated with the small thickness of the coating and the advantages of the magnetron technology.

CONCLUSIONS

Analysis of published and our own data led us to a conclusion that the technology of fabrication of optical coatings with a longitudinal gradient of refractive index has made a great progress. However, there are certain problems with, in particular, ensuring highly precise fabrication of refractive-index nanoprofiles at enhanced performance of the processes of deposition of gradient coatings. Therewith, a high resistance of the coatings to environmental factors should be provided.

Optical coatings with a longitudinal gradient of refractive index work in a wide range of light wavelengths and incidence angles. There is an urgent demand for such coatings for various-application optical system, optoelectronic and laser devices, optical elements with nanogradient metacoatings [39], and high-performance solar cells.

ACKNOWLEDGMENTS

The work was financially supported in part by the Ministry of Education and Science of the Russian Federation (State Contract no. 14.513.11.0098).

REFERENCES

1. Gomez-Reino, C., Perez, M.V., and Bao, C., *Gradient-Index Optics. Fundamentals and Applications*, Berlin: Springer, 2002.
2. Volpian, O.D., Kuzmichev, A.I., Obod, Yu.A., and Yakovlev, P.P., *Materialy 15-i nauchn.-tekhn. konf. "Vysokie tekhnologii v promyshlennosti Rossii* (*Materialy i ustroistva funktsional'noi elektroniki i mikrofotoniki)"* (Proc. 15th Scientific Technical Conf. "High Technologies in Russian Industry (Materials and Devices for Functional Electronics and Microphotonics), Moscow, 2009, pp. 447–450.
3. Movchan, B.A., *Surf. Coat. Technol*., 2002, vol. 149, pp. 252–262.
4. Movchan, B.A. and Yakovchuk, K.Yu., *Ibid*., 2004, vols. 188–189, pp. 85–92.
5. Lozovan, A.A. and Shchitov, N.N., *Tekhnol. Mashinostr*., 2007, no. 9. pp. 36–39.
6. *PLATIT. Gradient Coating. Nanogradients. http:// www.platit.com*.
7. *VNIIInstrument. Nanogradientnye pokrytiya iz separativnoi plazmy dugovogo razryada* (Russian Research & Development Tooling Institute. Nanogradient Coatings from Separated Arc Discharge Plasma); *http://www.vniiinstrument.ru/production.*
8. Southwell, W.H., *Opt. Lett*., 1983, vol. 8, pp. 584–586.
9. Kim, J.H. and Lee, Y.J., *J. Opt. Soc. Korea*, 2000, vol. 4, pp. 86–88.

10. Macleod, H.A., *Thin-Film Optical Filters*, Boca Raton, FL: CRC Press, 2010.
11. Janicki, V., Gäbler, D., Wilbrandt, S., et al., *Appl. Opt*., 2006, vol. 45, pp. 7851–7857.
12. Janicki, V., Sancho-Parramon, J., Stenzel, O., et al., *Ibid*., 2007, vol. 46, pp. 6084–6091.
13. Ouellette, M.F., Lang, R.V., Yan, K.L., et al., *J. Vac. Sci. Technol. A*., 1991, vol. 9, pp. 1188–1192.
14. Jankowski, A.F., Schrawyer, L.R., and Perry, P.L., *J. Vac. Sci. Technol. A*., 1991, vol. 9, pp. 1184–1187.
15. Qiu,W., Kang, Y.Mo, and Goddard, L.L., *Appl. Phys. Lett*., 2010, vol. 96, p. 141116 (1–3).
16. Xi, J.-Q., Kim, J.K., Schubert, E.F., et al., *Opt. Lett.,* 2006, vol. 31, pp. 601–603.
17. Poxson, D.J., Schubert, M.F., Mont, F.W. et al., *Ibid.*, 2009, vol. 34, pp. 728–730.
18. Kuo, M.-L., Poxson, D.J., Kim, Y.S., et al., *Ibid*., 2008, vol. 33, pp. 2527–2529.
19. Kennedy, S.R. and Brett, M.J., *Appl. Opt*., 2003, vol. 42, pp. 4573–4579.
20. Li, B.X., Gao, J., Xue, L., and Han, Y., *Adv. Funct. Mater*., 2010, vol. 20, pp. 259–265.
21. Martinu, L. and Poitras, D., *J. Vac. Sci. Technol. A*., 2000, vol. 18, pp. 2619–2645.
22. Poitras, D., Stephane, S., and Martinu, L., *Appl. Opt*., 2002, vol. 41, pp. 5249–5255.
23. Stephane, S., Szymanowski, H., Klemberg-Sapieha, J.E., et al., *J. Vac. Sci. Technol. A*, 2004, vol. 22, pp. 1200–1207.
24. Callard, S., Gagnaire, A., and Joseph, J., *J. Vac. Sci. Technol. A*, 1997, vol. 15, pp. 2088–2094.
25. Jacobsson, R., *Physics of Thin Films*, Hass, G., Francombe, M.H., and Hoffman, R.W., Eds., New York: Academic, 1975, vol. 8, p. 51–98. Translated under the title *Fizika tonkikh plenok*, Moscow: Mir, 1978, pp. 61–105.
26. Gunning, W.J., Hall, R.L., Woodberry, F.J., et al., *Appl. Opt*., 1989, vol. 28, pp. 2945–2948.
27. Lambrinos, M.F., Valizadeh, R., and Colligon, J.S., *Nucl. Instr. Meth. Phys. Res. B*, 1997, vol. 127–128, pp. 369–374.
28. Snyder, P.G., Xiong, Yi-M., Woollam, J.A., et al., *J. Vac. Sci. Technol. A*. 1992, vol. 10, pp. 1462–1466.
29. Leitel, R., Stenzel, O., Wilbrandt, S., et al., *Thin Solid Films*, 2006, vol. 497, pp. 135–141
30. Chao, S., Chang, C.-K., and Chen, J.-S., *Appl. Opt*., 1991, vol. 30, pp. 3233–3237.
31. Ritz, A., *Surf. Coat. Technol*., 2003, vols. 174–175, pp. 651–654.
32. Tang, Q., *Ogura S. J. Vac. Sci. Technol. A.,* 1997, vol. 15, p. 2670–2672.
33. Song Y., Sakurai, T., Maruta, K., et al., *Vacuum,* 2000, vol. 59, pp. 755–763.
34. Bartzsch, H., Frach, P., Goedicke, K., and Gottfried, Chr., *Surf. Coat. Technol*., 1999, vol. 120-121, pp. 723–727.
35. Bartzsch, H., Lange, S., Frach, P., and Goedicke, K., *Ibid*., 2004, vol. 180-181, p. 616–620.
36. Lange, S., Bartzsch, H., Frach, P., and Goedicke, K., *Thin Solid Films*, 2006, vol. 502, pp. 29–33.
37. Weber, J., Bartzsch, H., and Frach, P., *Appl. Opt*., 2008, vol. 47, pp. 288–292.
38. Shvartsburg, A.B., Agranat, M.B., and Chefonov, O.I., *Quantum Electron*., 2009, vol. 39, pp. 948–952.
39. Volpian, O.D. and Kuzmichev, A.I., *Otritsatel'noe prelomlenie voln. Vvedenie v fiziku i tekhnologiyu elektromagnitnykh metamaterialov* (Negative Refraction of Waves. Introduction to Physics and Technology of Electromagnetic Metamaterials), Kiev: Avers, 2012.